IRIS AperTO

UNIVERSITÀ DEGLI STUDI DI TORINO

AperTO - Archivio Istituzionale Open Access dell'Università di Torino

Squaraine Dyes: Interaction with Bovine Serum Albumin to Investigate Supramolecular Adducts with Aggregation-Induced Emission (AIE) Properties

This is a pre print version of the following article:

Original Citation:

Availability:

This version is available http://hdl.handle.net/2318/1695308 since 2020-02-19T16:07:09Z

Published version:

DOI:10.1002/asia.201900055

Terms of use:

Open Access

Anyone can freely access the full text of works made available as "Open Access". Works made available under a Creative Commons license can be used according to the terms and conditions of said license. Use of all other works requires consent of the right holder (author or publisher) if not exempted from copyright protection by the applicable law.

(Article begins on next page)

15 September 2026

Squaraine dyes: interaction with bovine serum albumin to investigate supramolecular adducts with aggregation-induced emission (AIE) properties

Nadia Barbero,[a] Cosmin Butnarasu,[b] Sonja Visentin[b] and Claudia Barolo[a]*

[a] Dr. N. Barbero, Prof. C. Barolo

Department of Chemistry, NIS Interdepartmental and INSTM Reference Centre, University of Torino, Via Pietro Giuria 7, 10125 Torino, Italy

E-mail: claudia.barolo@unito.it

[b] C. Butnarasu, Dr. S. Visentin

Department of Molecular Biotechnology and Health Sciences, University of Torino, via Quarello 15A, 10135 Torino, Italy

Abstract

Bovine Serum Albumin (BSA)–squaraine supramolecular adducts with aggregation-induced emission (AIE) properties were prepared and characterized by spectroscopic methods. While squaraine dyes showed very low fluorescence quantum yield in water, a great enhancement in the fluorescence of the aggregated BSA adducts was achieved due to the abnormal aggregation-induced emission properties of squaraines. The adducts formation was studied from a kinetic point of view showing unexpected structure-properties relationships.

Introduction

Serum albumin is the major protein in blood plasma and has been extensively studied because of its availability, low cost, stability and unusual ability to bind and transport various ligands to specific sites.[1] Its ligand binding properties towards a variety of endogenous and exogenous substances in blood is due to the existence of a limited number of binding regions of very different specificity. The two major binding sites are selective and dominated by strong hydrophobic interactions (site I) and by a combination of hydrophobic, electrostatic interactions and hydrogen bonding (site II). Moreover, it has been reported that drugs with preferential affinity towards binding site II show efficient photodynamic therapeutic applications.[2] In order to use albumin as a tumor targeting carrier, a moderate binding between the protein and the drug is required.[3] Then, along with the potency of drug-target binding interactions measured by the Kd, binding kinetics is undoubtedly an essential issue in drug discovery. Both residence time and association rate constant are important parameters for in vivo efficacy and safety of drugs since they can help in understanding their mechanisms of action and structure-activity relationships.[4]

A great number of studies involving protein-dye interactions have been published so far[5] since the interest in developing new probes that can noncovalently bind proteins for their detection and sensing is constantly growing. In particular, several fluorescent compounds (such as cyanine dyes and squaraine dyes[6,7]) exhibit a fluorescence “turn on” when bound to proteins which translate into an increase in quantum yield and lifetime due to the changes in the environment. Squaraines are poorly soluble in aqueous media, and the consequent easy formation of non-fluorescent aggregates heavily limited their use as fluorescent markers for biological applications.[8] A great enhancement in the fluorescence of the aggregated BSA adducts was achieved due to aggregation-induced emission (AIE).

AIE is a novel photophysical phenomenon found in a group of luminogens that are non-fluorescent in solution but are highly emissive in the aggregate or solid state.[9,10] AIE is a unique photophysical phenomenon associated with chromophore aggregation. Fluorogens with aggregation-induced emission characteristics have recently emerged as a new class of fluorescent bioprobes for biosensing[11,12] and cell imaging.[13,14] Instead of fluorescence quenching, the emission of luminogens with AIE characteristics is turned on when they are aggregated. Suzuki and Yokoyama noticed a colour change of a squaraine dye upon complexation with BSA[15] while the group of Ramaiah showed a huge enhancement in fluorescence quantum yields for a squaraine binding to BSA.[7] Few years later, the same group demonstrated that steric factors of the substituents can strongly influence the binding of squaraines with serum albumins.[6] Volkova et al. also tried to study the influence of the dyes structures (a series of squaraines) on the selectivity towards different proteins (BSA, human serum albumin, ovalbumin and avidin).[16] The squaraine "turn on" fluorescence upon association with BSA[17] can be attributed to a change in environment after complexation with BSA.[18] This was deeply studied by Gao et al.[19] who attributed this effect to the release of the squaraine dye from the non-fluorescent H-aggregates by the formation of a squaraine-protein adduct. It is therefore evident that there is an urgent need and challenge for the development of novel fluorescent probes to serve as a platform for a variety of applications and these adducts are very interesting since they can be used as effective bioimaging probes or as sensors[20,21], as photothermal absorber agents with improved photodestruction efficacy[19] or for photoacoustic tomography.[22] Moreover, BSA-dyes adducts can be of the utmost importance for the preparation of protein biophosphors for white emission, sensing and pH detection,[23] Solid-state lighting (SSL) based on Biological Materials,[24] detection and quantitation of ions[12,17,25] and other species in blood serum or the development of bio-hybrid white LEDs (Bio-HWLEDs).[26]

In this scenario, since the importance of these adducts, in the present paper we show our results on a thermodynamic and kinetic study undertaken on the interaction between BSA and a series of squaraine dyes, with different substitutions. We selected four squaraine dyes differing from the nature of the lateral indolenine or benzoindolenine group and the length of the alkyl chain (see Figure 1). We studied the interaction by means of steady-state and stopped-flow fluorescence emission intensity to evaluate the thermodynamic and kinetic binding parameters.

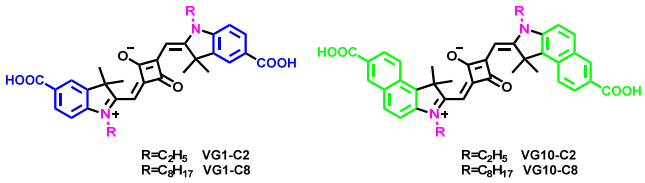

Figure 1. Structures of the squaraine dyes used.

Results and Discussion

UV-Vis and Steady-state fluorescence spectroscopy

The interaction between each dye and BSA was first checked by UV-Vis spectroscopy (Figure 2). VG1-C2 showed a decrease of the absorption upon addition of increasing concentration of BSA with a bathochromic shift of 3-4 nm while the analogue squaraine dye with longer alkyl chains, VG1-C8, showed an increase of absorption with a more consistent bathochromic shift (14 nm) upon the formation of the squaraine-BSA complex. A very similar behavior (Abs increase and red shift of 13 nm) was registered for VG10-C2, which differs from VG1-C2 from the presence of a benzoindolenine group instead of an indolenine group on the lateral substituent. A completely different scenario appears for VG10-C8, characterized by a bulkier group and longer alkyl chains that shows some solubility issues in water with the formation of aggregates as evidenced in Figure 2d.

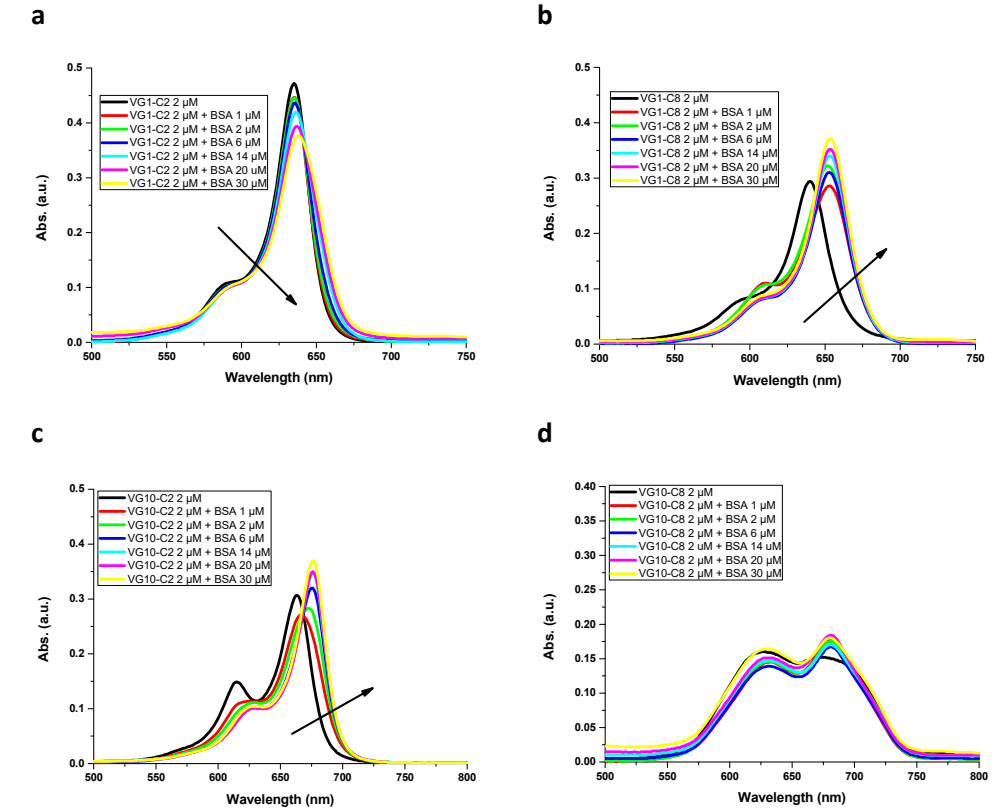

Figure 2. UV-Vis absorption change of VG1-C2 (a), VG1-C8 (b), VG10-C2 (c) and VG10-C8 (d) upon addition of BSA.

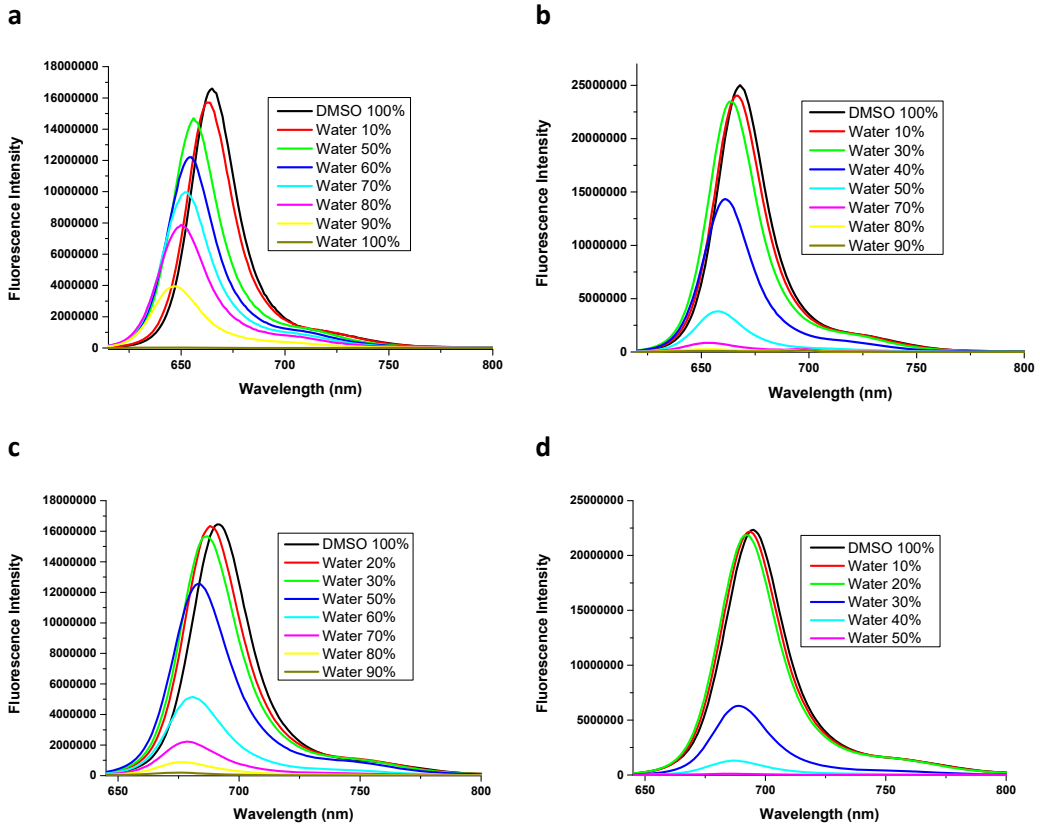

Figure 3. Steady-state fluorescence intensity change of VG1-C2 (a), VG1-C8 (b), VG10-C2 (c) and VG10-C8 (d) in DMSO upon addition of water.

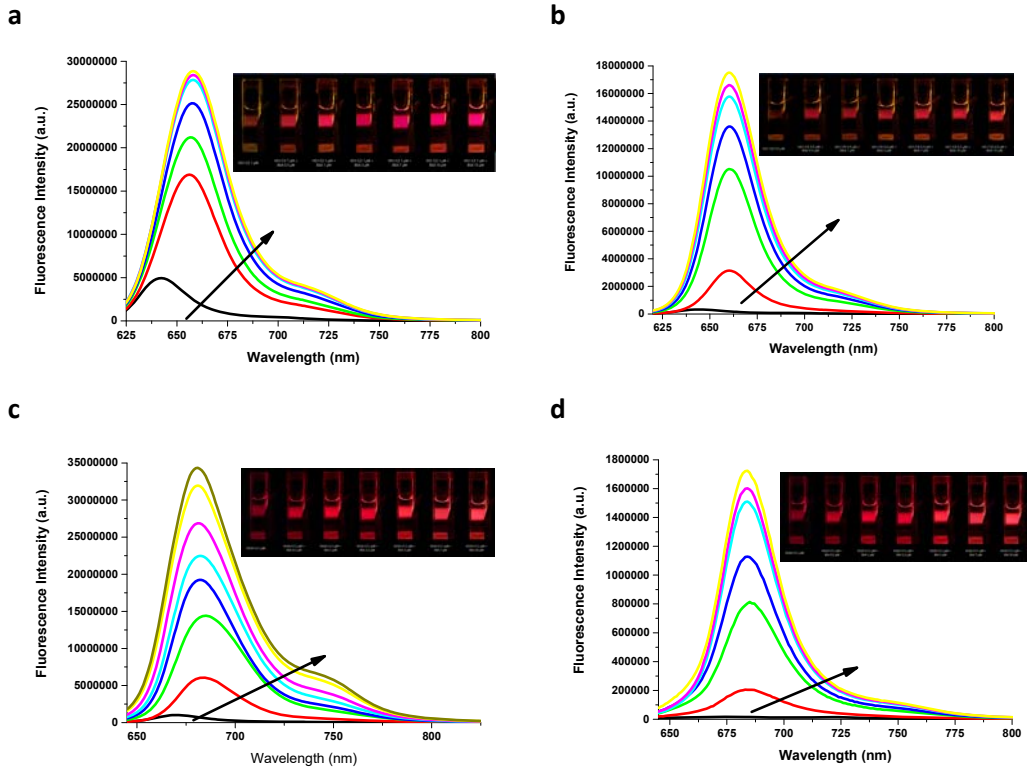

Figure 4. Steady-state fluorescence intensity change of VG1-C2 (a), VG1-C8 (b), VG10-C2 (c) and VG10-C8 (d) upon addition of BSA.

All the studied squaraines showed excellent emission properties in organic solvents but a poor emission when PBS buffer amount increased due to an aggregation caused quenching (ACQ) effect (Figure 3). Actually, it is well known and deeply described in literature that, when the squaraine alone is in a water solution, it tends to form non-fluorescent aggregates.[18,27] One of these squaraines, i.e. VG1-C8, already showed, in solid state, micron-sized polycrystalline aggregate exhibiting a large Stokes shift (322 nm).[28] Squaraine molecules are almost non-emissive when they are dissolved in water but are bright emitters in the solid state[28] or in an aggregate state when the supramolecular adduct is formed. On the contrary, in 100% PBS buffer, a gradual addition of BSA gave an enhancement in fluorescence intensity with a bathochromic shift of about 11-12 nm for all the studied squaraines (Figure 4). The formation of an aggregate is confirmed by the bathochromic shift recorded for the SQ-BSA adduct. Moreover, the UV band shift and fluorescence intensity increase can be attributed to an AIE effect due to the formation of the aggregate between squaraine and BSA. Upon addition of the squaraine solution into the BSA solution, squaraine molecules aggregate and may entangle with the hydrophobic segments of the BSA chains. The subsequent additions also yielded a significant change in fluorescence emission up to a 11-fold enhancement in fluorescence quantum yield (QY) for VG1-C8 and VG10-C2 (see Table 1). The obtained quantum yield in PBS buffer are comparable with the QY obtained in tetrahydrofuran and higher than the ones obtained in more polar solvents.[29,30] To have a better insight of the origin of this fluorescence enhancement, we compared the QY obtained in water with the values obtained in organic solvents with different polarity[30] as proposed by Gao et al.[19]. When water was added into DMSO solutions of SQ a rapid decrease of the fluorescence quantum yield was given (0.03 with 100% water). This behavior is due to the formation of non-fluorescent SQ H-aggregates in water. The fluorescence enhancement, in presence of BSA, has to be attributed to the release of SQ dye from the non-fluorescent H-aggregates by adduct formation of SQ-BSA aggregates as evidenced by TEM analysis.

The emission properties and fluorescence QY are constant even after lyophilization and subsequent solubilization in water. The water solution of the complex can be stored for days without any particular precautions.

Table 1. Absorbance and emission maxima and quantum yields of the studied squaraines, in PBS buffer, in absence and presence of BSA

Dye	λ_{abs} nm	λ_{em} nm	Φ		λ_{abs} nm	λ_{em} nm	Φ
VG1-C2	635	644	0.03	+BSA	637	655	0.21
VG1-C8	640	648	0.05	+BSA	654	661	0.56
VG10-C2	663	674	0.05	+BSA	676	685	0.54
VG10-C8	674	674	0.04	+BSA	681	686	0.29

Transmission electron microscopy

In order to obtain direct evidence on complex formation, morphological analysis was performed using TEM.

The experiment was performed on a SQ-BSA solution. The complex solution was not purified to avoid the presence of free protein since we work with a SQ excess. Fig. 5 shows the images obtained for the complex SQ-BSA revealing the presence of aggregates of around 200-300 nm.

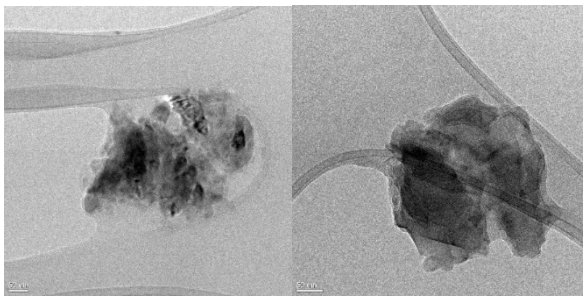

Figure 5. Images of complex SQ-BSA seen under the transmission electron microscope with a magnification of ×30,000 (left) and ×40,000 (right).

Kinetic results of squaraines interaction with BSA

To have a better understanding of the interaction of the four squaraine dyes with BSA, we carried out time-resolved and kinetics fluorescence studies. We started with VG1-C2 and the maximum values of the complex fluorescence intensity were plotted in Figure 6 against the increasing BSA concentration and fitted by a hyperbole equation giving the following dissociation and association binding constants, respectively, KD = 1.6·10-6 M ± 4.9·10-7 and KA = 6.4·105 M-1.

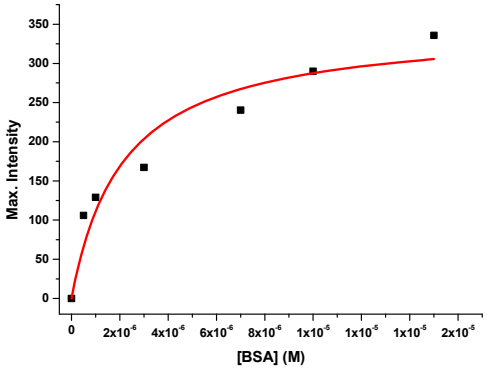

Figure 6. Intensity maxima obtained at various BSA concentration (0, 0.5, 1, 3, 7, 10 and, 20µM) for the monitoring of the VG1-C2/BSA complex formation. The red curve in the figure is the fitting to a hyperbole equation for the evaluation of the binding constant.

The complex formation between VG1-C2 and BSA was further confirmed by time-correlated single photon counting (TCSPC). Time-resolved fluorescence analysis indicated that VG1-C2 alone exhibits a mono-exponential decay, whereas bi-exponential decay with significantly increased lifetimes were observed in the presence of BSA (Figure S1).

To get more insights into the interaction between VG1-C2 and BSA, we also examined the kinetic interaction of the binding by stopped flow fluorescence. The binding was investigated under pseudo-first order condition[31] ([BSA]>>[VG1-C2]) by monitoring the fluorescence changes after the formation of the complex. Figure 7a shows that on mixing 1 mM BSA with 30 mM SQ (cell concentration) there is an increase of the signal which reaches a plateau after few ms. Raw data were analyzed and plotted to a double exponential function.

The interaction was studied by keeping squaraine concentration fixed at 0.5 µM and changing the BSA concentration. The dependence of the observed rate constant (kobs) of VG1-C2 binding to BSA (BSA concentration over a range of 0.5–55 µM) is shown in Figure 6b. As is evident, the dependence is linear and thus the values of the kinetic parameters can be calculated from the slopes and intercepts of linear plots of kobs versus the increasing concentration of BSA (see eqn 1).

$$kobs=k+1[BSA]+k-1 \qquad (1)$$

In particular, the slope of the straight line is the kon (second order rate constant; units, M-1s-1) and the intercept on the ordinate is the koff (first-order rate constant; units, s-1). The second-order rate constant kon is evaluated as 8.0·106 M-1 s-1 and the Koff as 15.6 s-1, giving a KA= 5.1·105 M-1 and a KD = 1.9·10-6 M, in very good agreement with the thermodynamic binding constants obtained by the fluorescence steady-state experiment. The linear trend shown in Figure 7b also suggests that the interaction occurs in a single step.

a **b**

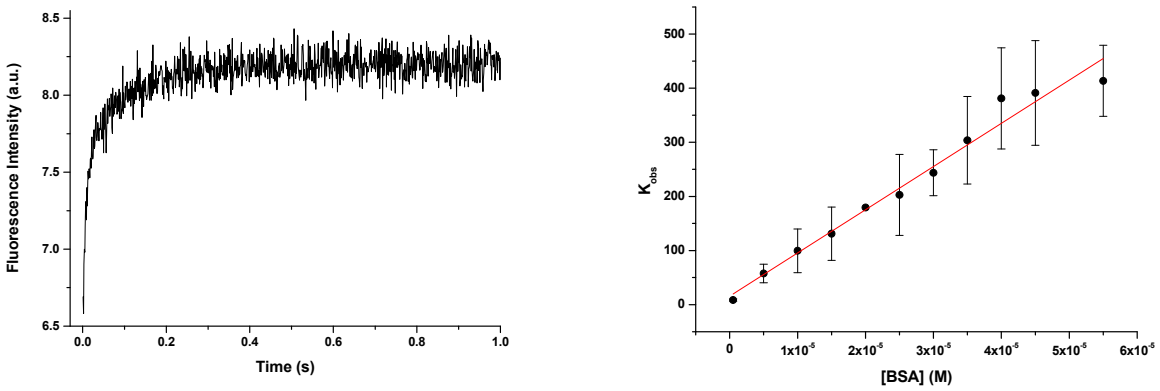

Figure 7. (a) The stopped-flow fluorescence intensity record of the binding of 0.5 µM VG1-C2 to 30 µM BSA and (b) The dependence of the kobs determined by stopped-flow fluorescence intensity. Data points are the mean of ten independent experiments, standard deviation is also reported. In two points, error bar is not visible as it is concealed by the data point.

Since it is important to understand not only how much squaraine is bound to the protein but also the site-specificity of the binding, a site-specific fluorescent probe technique was used to understand the site-selective binding of the squaraines tested with BSA. We employed fluorescence probe displacement experiments using known site-selective binding ligands, such as indomethacin (for site I) and ibuprofen (IB, for site II).

Addition of IB to a solution of BSA (14µM)/VG1-C2 (6µM) complex resulted in a gradual decrease of fluorescence intensity (Figure S2) and then reached saturation at 0.5 mM of IB. A similar procedure was applied using indomethacin to check site I: it showed ability to displace VG1-C2 (Figure S3), thus indicating that VG1-C2 interacts with BSA at site I and II, in agreement with the double exponential fitting of the stopped-flow data.

We performed the same binding experiments with BSA also for the other squaraine dyes reported in Figure 1. While performing the titration experiment to evaluate binding constants, we noticed that the intensity signal for all the other three complexes (i.e. VG1-C8/BSA, VG10-C2 and VG10-C8) was not stable. Thus, we decided to perform a time-drive experiment for 50 minutes, with scans every 0.01 minutes.

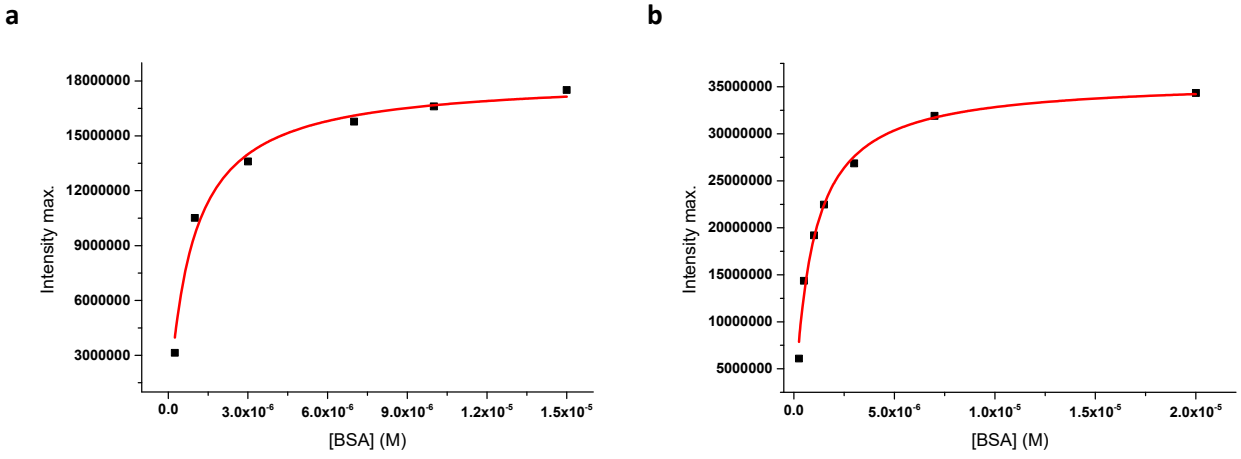

Figure 8. Intensity maxima obtained at various BSA concentration for the monitoring of the (a) VG1-C8/BSA and (b) VG10-C2 complex formation. The red curve is the fitting to a hyperbole equation for the evaluation of the binding constant.

The VG1-C8/BSA complex reaches a plateau after about 45 min (see Figure S4). The maximum intensity values obtained were plotted versus the increasing BSA concentration and fitted to a hyperbola equation, as in the case of VG1-C2/BSA complex, obtaining a dissociation binding constant KD of 8.9·10-7 M ± 1.3·10-7 (Figure 8a). We can then observe that the increase of the length of the alkyl chain on the indolenine moieties has a great influence on both the thermodynamics and kinetics of the complex formation: the binding constants differ from one order of magnitude and the kinetics results faster for the short length chain dye VG1-C2. The interaction for VG10-C2/BSA reaches a plateau after 25 minutes (see Figure S5): this intensity value was used for the calculation of the binding constants, again obtained by fitting the points in Figure 8b using the hyperbola equation obtaining a KD of 8.9·10-7 M ± 8.5·10-8. These two squaraine dyes have a very similar thermodynamic and kinetic behavior with very similar binding constants differing from VG1-C2. A summary of the different kinetic behavior for the four complex formation is depicted in Figure 9.

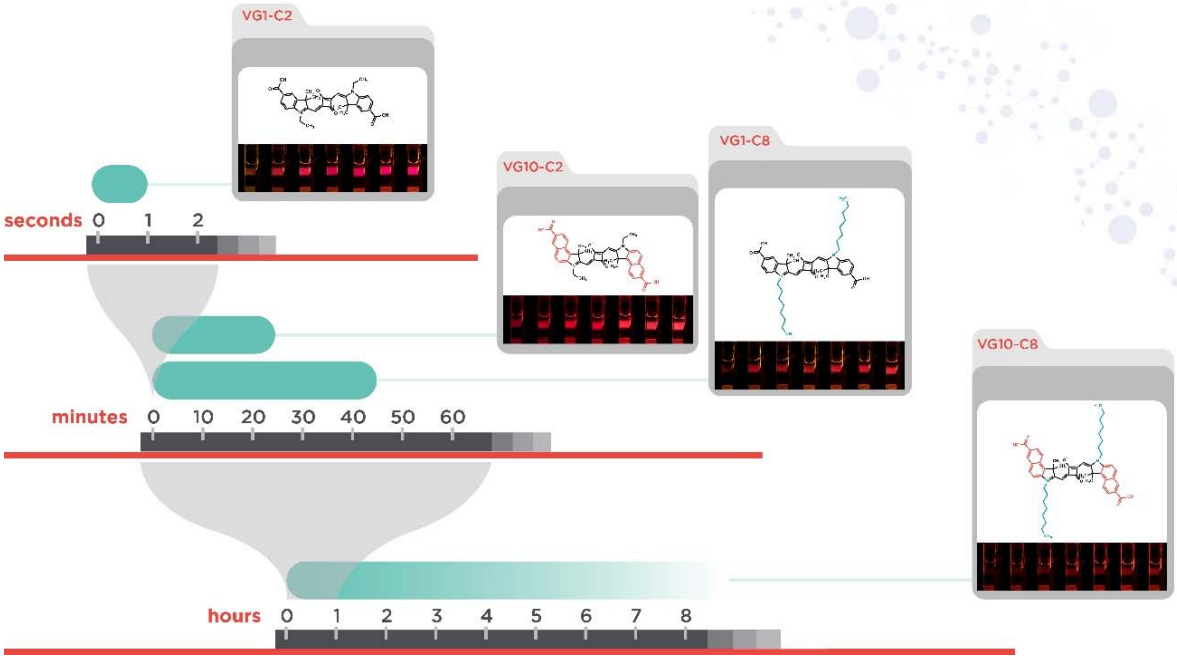

Figure 9. Kinetic behavior of the four complex formation.

The same approach was followed for the benzoindolenine-based dye with long chain, i.e. VG10-C8, but in this case it was impossible to reach the equilibrium of the interaction even after 6 hours (see Figure S6). The time-drive experiment was performed for 20 hours, with scans every 0.15 minutes. Since the waiting time was too long, we did not investigate the interaction further. The presence of a bulkier group (benzoindolenine versus indolenine) and longer chains (C8 vs C2) greatly influences the kinetic of the system. The experimental results clearly show that the response time is affected by the structure of the squaraine. The presence of smaller indolenine group compared to the bulkier benzoindolenine has an effect on the kinetic of interaction (i.e. VG1 vs VG10). VG1 interaction with BSA is faster than VG10-BSA interaction. For example, VG1-C2 interaction with BSA occurs in a ms time scale while the interaction between VG10-C2 and BSA takes 25 minutes. Moreover, also the presence of longer alkyl chains plays a crucial role on the kinetic of the interaction (i.e. C2 vs C8). In fact, VG1-C8/BSA takes around 45 minutes to occur compared to few ms time scale for VG1-C2. Moreover, as already demonstrated in our previous work,[2] also in this case, BSA complexes with similar thermodynamic binding constants show a very different behavior from a kinetic point of view. It is also evident that the kinetic of the interaction has a great influence on AIE phenomenon: for fast kinetic the fluorescence enhancement is more pronounced (i.e. VG1-C2) while it is less evident for long lasting interactions (i.e. VG10-C8). It seems obvious that the

adducts formation is influenced not only by the steric hindrance of the molecules but also by their degree of lipophilicity demonstrating an unexpected structure-properties relationships.

Conclusions

We reported a thermodynamic and kinetic study of the formation of supramolecular adducts between a series of squaraine dyes and bovine serum albumin. Squaraine dyes showed a structure–relationship influence on the kinetic interaction with serum albumins with a significant fluorescence intensity enhancement. Upon addition of the squaraine solution into the BSA solution, squaraine molecules aggregate and may entangle with the hydrophobic segments of the BSA chains. Actually, the fluorescence quantum yields of the SQ-BSA adducts in buffer are comparable with the ones reported in organic solvents. These results make these adducts very interesting as potential probes or photosensitizers for different applications (bioimaging, photodynamic therapy…). We noticed that the dye backbone structure as well as the length of the alkyl chain play a crucial role on the kinetic of the interaction. Thus, the right choice of the structure of the probe can be used to modulate the AIE effect that can be required depending on the biological applications.

Experimental Section

Materials

All reagents were of analytical reagent grade and double distilled water was used. BSA solutions were prepared based on its molecular weight of 66,000. Squaraine dyes were prepared as previously described.[32] BSA mother solution (1 mM) was prepared in PBS buffer (2 mM, pH 7.4). Mother solutions of the dyes (1 mM) were prepared in DMSO. Dilutions for the experiments were performed in PBS buffer.

Methods

UV-Vis absorption spectroscopy

UV-VIS electronic absorption spectra were measured by a Cary 300 Bio spectrophotometer (Varian, Santa Clara, CA, USA), using quartz cuvettes (1 cm pathway length). Squaraine dyes concentration (2 µM in PBS buffer pH 7.4) was kept constant and BSA was changed over the range 1-30 µM in PBS buffer.

Emission spectroscopy

Fluorescence emission spectra in steady state mode were acquired using a Horiba Jobin Yvon Fluorolog 3 TCSPC fluorimeter equipped with a 450-W Xenon lamp and a Hamamatsu R928 photomultiplier.

Fluorescence spectra were recorded in the range of 615-850 nm for VG1-C2 and VG1-C8 and in the range of 645-850 nm for VG10-C2 and VG10-C8. Samples were excited at the squaraine hypsochromic shoulder of Abs: 595 nm for VG1-C2 and VG1-C2/BSA, 600 nm for VG1-C8 and 615 nm for VG1-C8/BSA, 625 nm for VG10-C2, VG10-C2/BSA, VG10-C8, VG10-C8/BSA. Squaraine dyes concentration (1 µM in PBS buffer pH 7.4) was kept constant and BSA was changed over the range 1-15 µM in phosphate buffer. For VG1-C8, VG10-C2 and VG10-C8 fluorescence experiments were also performed in a time drive mode in order to check whether and when the solution reached the stability. Fluorescence intensity was recorded every 60 s.

Fluorescence lifetimes were measured by the time correlated single photon counting method (Horiba Jobin Yvon) using a 560 nm Horiba Jobin Yvon NanoLED as excitation source and an impulse repetition frequency of 1 MHz positioned at 90° with respect to a TBX-04 detector. Lifetimes were calculated using DAS6 decay analysis software.

The absolute quantum yield was determined by means of an integrating sphere combining Quanta-ϕ with Fluorolog 3. The reported quantum yields are the average of the values obtained after three measurements using three different dye solutions.

Stopped flow fluorescence

Fluorescence kinetics measurements were recorded using an Applied Photophysics SX20 stopped-flow spectrometer fitted with a 610 nm cut-off filter between the cell and fluorescence detector and equipped with a thermostat bath (25 °C). Data acquisition, visualization, and analysis were provided by Pro-Data software from Applied Photophysics Ltd.

VG1-C2 concentration was kept constant (0.5 μM in PBS buffer pH 7.4) and several shots of different BSA concentrations were performed over the range 0.5–55 μM in phosphate buffer. Each experiment (whole concentration set) was repeated five times, each time using new mother solutions of BSA and VG1-C2. For each dilution condition at least five scans were acquired and averaged. Each experimental point is therefore, an average of 25 shots. Raw data were analysed and plotted to a double exponential function by using Pro-Data Viewer 4.0.17 and from this data treatment the observed rate constants (kobs) were obtained. The excitation wavelength was 580 nm and slits widths of the excitation monochromator were 1.5 mm.

Displacement experiments

We previously checked that no interaction occurred between the probes and the tested squaraines. The titrations of indomethacin and ibuprofen (IB) with SQ alone showed negligible changes in emission properties, indicating that the changes observed with the BSA-SQ complex were mainly due to the displacement of SQ from the complex by the binding ligands (Figure S7-S8).

Transmission electron microscopy

High-resolution transmission electron micrographs were obtained with a JEOL 3010-UHR instrument operating at 300 kV, equipped with a 2 k×2 k pixels Gatan US1000 CCD digital camera. Samples of SQ-BSA complex in PBS were dried on a carbon-coated copper grid. The nominal magnification used to record the complex SQ-BSA were ×30000 and ×40000.

Acknowledgements

Authors acknowledge the financial support from the University of Torino (Ricerca Locale ex-60%, Bando 2018).

Keywords: Aggregation-induced emission (AIE) • squaraines • Bovine Serum Albumin (BSA) • supramolecular adducts • kinetics

References

[1] T. Peters, All About Albumin, Academic Press, San Diego, 1996.

[2] N. Barbero, S. Visentin, G. Viscardi, J. Photochem. Photobiol. A Chem. 2015, 299, 38–43.

[3] S. Onoe, T. Temma, Y. Shimizu, M. Ono, H. Saji, Cancer Med. 2014, 3, 775–786.

[4] P. J. Tonge, ACS Chem. Neurosci. 2018, 9, 29–39.

[5] N. Barbero, E. Barni, C. Barolo, P. Quagliotto, G. Viscardi, L. Napione, S. Pavan, F. Bussolino, Dye. Pigment. 2009, 80, 307–313.

[6] V. S. Jisha, K. T. Arun, M. Hariharan, D. Ramaiah, J. Phys. Chem. B 2010, 114, 5912–5919.

[7] V. S. Jisha, K. T. Arun, M. Hariharan, D. Ramaiah, J. Am. Chem. Soc. 2006, 128, 6024–6025.

[8] I. A. Karpenko, A. S. Klymchenko, S. Gioria, R. Kreder, I. Shulov, P. Villa, Y. Me, M. Hibert, D. Bonnet, Chem. Commun. 2015, 51, 2960–2963.

[9] H. Wang, E. Zhao, J. W. Y. Lam, B. Z. Tang, Mater. Today 2015, 18, 365–377.

[10] J. Mei, N. L. C. Leung, R. T. K. Kwok, J. W. Y. Lam, B. Z. Tang, Chem. Rev. 2015, 115, 11718–11940.

[11] Z. Wang, K. Ma, B. Xu, X. Li, W. Tian, Sci. China Chem. 2013, 56, 1234–1238.

[12] W. Li, D. Chen, H. Wang, S. Luo, L. Dong, Y. Zhang, J. Shi, B. Tong, Y. Dong, ACS Appl. Mater. Interfaces 2015, 7, 26094–26100.

[13] H. Gao, X. Zhao, S. Chen, Molecules 2018, 23, 1–20.

[14] L. Huang, L. Dai, J. Polym. Sci. Part A Polym. Chem. 2017, 55, 653–659.

[15] Y. Suzuki, K. Yokoyama, Angew. Chemie - Int. Ed. 2007, 46, 4097–4099.

[16] K. D. Volkova, V. B. Kovalska, A. L. Tatarets, L. D. Patsenker, D. V Kryvorotenko, S. M. Yarmoluk, Dye. Pigment. 2007, 72, 285–292.

[17] P. Liu, W. Li, S. Guo, D. Xu, M. Wang, J. Shi, Z. Cai, B. Tong, Y. Dong, ACS Appl. Mater. Interfaces 2018, 10, 23667–23673.

[18] Y. Zhang, X. Yue, B. Kim, S. Yao, M. V Bondar, K. D. Belfield, ACS Appl. Mater. Interfaces 2013, 5, 8710–8717.

[19] F. Gao, Y. Lin, L. Li, Y. Liu, U. Mayerhöffer, P. Spenst, J. Su, J. Li, F. Würthner, H. Wang, Biomaterials 2014, 35, 1004–1014.

[20] Y. Xu, Q. Liu, X. Li, C. Wesdemiotis, Y. Pang, Chem. Commun. 2012, 48, 11313–11315.

[21] G. Wang, W. Xu, Y. Guo, N. Fu, Sensors Actuators B. Chem. 2017, 245, 932–937.

[22] F. F. An, Z. J. Deng, J. Ye, J. F. Zhang, Y. L. Yang, C. H. Li, C. J. Zheng, X. H. Zhang, ACS Appl. Mater. Interfaces 2014, 6, 17985–17992.

[23] K. Benson, A. Ghimire, A. Pattammattel, C. V Kumar, Adv. Funct. Mater. 2017, 27, 1702955.

[24] E. Fresta, V. Fernández-Luna, P. B. Coto, R. D. Costa, Adv. Funct. Mater. 2018, 28, 1707011.

[25] Y. Hong, C. Feng, Y. Yu, J. Liu, J. W. Y. Lam, K. Q. Luo, B. Z. Tang, Anal. Chem. 2010, 82, 7035–7043.

[26] V. Fernandez-Luna, P. B. Coto, R. D. Costa, Angew. Chem. Int. Ed. Engl. 2018, 57, 8826–8836.

[27] A. J. McKerrow, E. Buncel, P. M. Kazmaier, Can. J. Chem. 1995, 73, 1605–1615.

[28] G. M. Paternò, L. Moretti, A. J. Barker, C. D'Andrea, A. Luzio, N. Barbero, S. Galliano, C. Barolo, G. Lanzani, F. Scotognella, J. Mater. Chem. C 2017, 5, 7732–7738.

[29] J. Park, N. Barbero, J. Yoon, E. Dell'Orto, S. Galliano, R. Borrelli, J.-H. Yum, D. Di Censo, M. Grätzel, M. K. Nazeeruddin, et al., Phys. Chem. Chem. Phys. 2014, 16, 24173–24177.

[30] J. Park, C. Barolo, F. Sauvage, N. Barbero, C. Benzi, P. Quagliotto, S. Coluccia, D. Di Censo, M. Grätzel, M. K. Nazeeruddin, et al., Chem. Commun. 2012, 48, 2782.

[31] N. Barbero, L. Napione, S. Visentin, M. Alvaro, A. Veglio, F. Bussolino, G. Viscardi, Chem. Sci. 2011, 2, 1804–1809.

[32] N. Barbero, C. Magistris, J. Park, D. Saccone, P. Quagliotto, R. Buscaino, C. Medana, C. Barolo, G. Viscardi, Org. Lett. 2015, 17, 3306–3309.